Journal of Nuclear Materials 389 (2009) 52–56

Contents lists available at ScienceDirect

Journal of Nuclear Materials

journal homepage: www.elsevier.com/locate/jnucmat

Eutectic crystallization in the $FeO_{1.5}$–UO_{2+x}–ZrO_2 system

V.I. Almjashev [a], M. Barrachin [b], S.V. Bechta [c], D. Bottomley [d], F. Defoort [e], M. Fischer [f], V.V. Gusarov [a], S. Hellmann [f], V.B. Khabensky [c], E.V. Krushinov [c], D.B. Lopukh [g], L.P. Mezentseva [a,*,1], A. Miassoedov [h], Yu.B. Petrov [g,2], S.A. Vitol [c]

[a] *Institute of Silicate Chemistry of Russian Academy of Sciences, Makarova Emb., 2, Saint-Petersburg 199034, Russian Federation*
[b] *Institut de Radioprotection et Sûreté Nucléaire (IRSN), BP 3 F-13115 St-Paul-Lez-Durance, France*
[c] *A.P. Aleksandrov Research Institute of Technology, Sosnovy Bor, 188540, Russian Federation*
[d] *EC, Joint Research Centre, Institute for Transuranium Elements, Postfach 2340, Hermann-von-Helmholtz-Pl. 1, 76125 Karlsruhe, Germany*
[e] *Laboratoire de Physico-Chimie et Thermohydraulique Multiphasiques (LPTM), CEA/Grenoble, DTN/SE2T/LPTM, 17 Rue des Martyrs, 38 054 Grenoble cedex 9, France*
[f] *AREVA NP GmbH, Paul-Gossen-Str. 100, 91058 Erlangen, Germany*
[g] *Saint-Petersburg Electrotechnical University 'LETI', Prof. Popova Str., 5, Saint-Petersburg 197376, Russian Federation*
[h] *Forschungszentrum Karlsruhe, IKET, P.O. Box 3640, 76021 Karlsruhe, Germany*

ABSTRACT

Results of the investigation of the $FeO_{1.5}$–UO_{2+x}–ZrO_2 system in air are presented. The eutectic position and the content of the phases crystallized at this point have been determined. The temperature and the composition of the ternary eutectic are 1323 ± 7 °C and 67.4 ± 1.0 $FeO_{1.5}$, 30.5 ± 1.0 UO_{2+x}, 2.1 ± 0.2 ZrO_2 mol.%, respectively. The solubilities of $FeO_{1.5}$ and ZrO_2 in the $UO_{2+x}(FeO_{1.5}, ZrO_2)$ solid solution correspond to respectively 3.2 and 1.1 mol.%. The solubilities of UO_2 and ZrO_2 in $FeO_{1.5}$ are not significant. The existence of a solid solution on the basis of $U(Zr)FeO_4$ compound is found. The ZrO_2 solubility in this solid solution is 7.0 mol.%.

1. Introduction

The information on phase equilibria in the $FeO_{1.5}$–UO_{2+x}–ZrO_2 system is important for the analysis of physicochemical phenomena of a late phase nuclear power plant (NPP) severe accident involving corium interaction with structural materials, particularly, in oxidizing conditions [1–3]. The data on solidus and liquidus surfaces location in the $FeO_{1.5}$–UO_{2+x}–ZrO_2 system (mainly at the eutectic temperature) are important for the description of in-vessel corium melt behaviour and ex-vessel melt retention and crystallization in a core catcher [4,5]. The phase diagram of the ternary system is not yet fully determined and only limited data are available in the past literature [6]. For that reason any new experimental data could be potentially used for optimization of thermodynamic databases [7] that are applied in severe accident modeling.

The UO_2–Fe_3O_4–O system was investigated in [8]. In particular, the polythermal UO_{2+x}–Fe_2O_3 section was studied, for which the eutectic point was determined (1348 °C, 37.3 mol.% UO_2) and the liquidus line was constructed up to ∼1400 °C in this work (Fig. 1(a)). According to [8–10], Fe_2O_3 decomposes in air at temperatures higher than 1380 °C forming Fe_3O_4. In contact with uranium oxide (UO_{2+x}) the thermal stability of Fe_2O_3 increases [8]. This can indirectly prove the formation of $Fe_2O_3(UO_{2+x})$ solid solution. The phase diagram of the UO_{2+x}–Fe_2O_3 system in air atmosphere was constructed in [11], however the determined eutectic point (1240 ± 10 °C, 41 mol.% UO_2) distinctly differs from the data published in [8] (Fig. 1). According to [12–16], the $FeUO_4$ and FeU_3O_{10} compounds can exist in the UO_{2+x}–Fe_2O_3 system, affecting the solidus and liquidus surface location in the $FeO_{1.5}$–UO_{2+x}–ZrO_2 system.

The ZrO_2–Fe_2O_3 system in air atmosphere was investigated in [17]. The eutectic point was found to be at 1525 °C and 13.5 mol.% ZrO_2 (Fig. 2(a)), but obviously corresponded to phase equilibrium in the ZrO_2–Fe_3O_4 system due to hematite decomposition. The composition range was limited by a Fe_2O_3-enriched domain. It should be pointed out that the liquidus temperatures in the high-temperature domain and the component mutual solubility in solid state were not determined in [17]. Liquidus line extrapolation from the eutectic point up to ZrO_2 melting temperature and prediction of the possible solubility limits of Fe_2O_3 in ZrO_2 were only presented (Fig. 2(a)). Phase relations in the high-temperature range of the ZrO_2–FeO–Fe_2O_3 system were studied in [18,19]. According to these works, a miscibility gap in this ternary system is possible (Fig. 2(b)).

The data on component mutual solubility and unit cell parameter variation of solid solutions in the Fe_2O_3–ZrO_2 system are pre-

---

[*] Corresponding author. Tel.: +7 812 325 41 36; fax: +7 812 328 85 89.
E-mail address: la_mez@mail.ru (L.P. Mezentseva).

[1] Present address: ul. Karbysheva, d. 10, kv. 108, Saint-Petersburg 194021, Russia.

[2] Deceased.

0022-3115/$ - see front matter © 2009 Elsevier B.V. All rights reserved.
doi:10.1016/j.jnucmat.2009.01.006

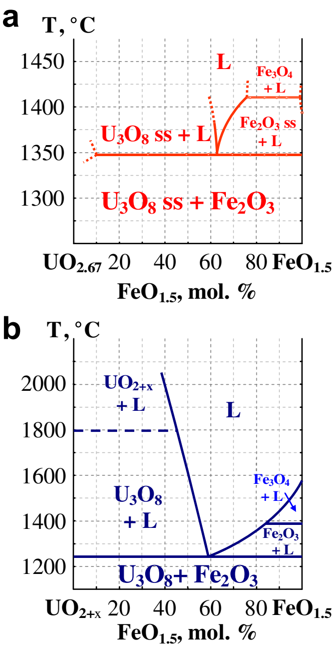

Fig. 1. Phase diagrams of the UO_{2+x}–$FeO_{1.5}$ system in air. Literature data: (a) [8], (b) [11].

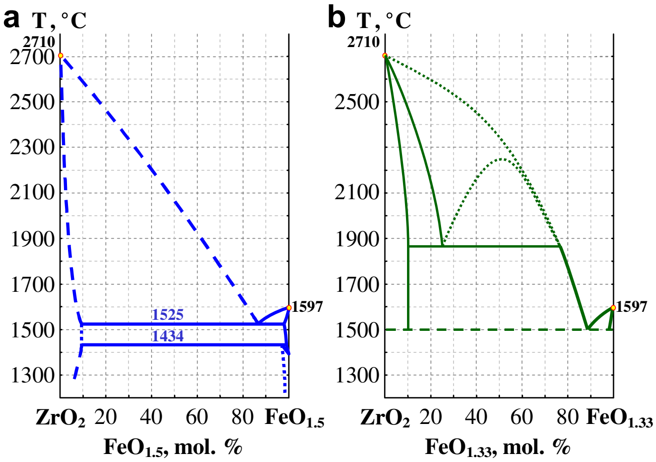

Fig. 2. Phase diagrams of the ZrO_2–$FeO_{1.5}$ system in air. Literature data: (a) [17], (b) [19].

sented in [20]. Formation of solid solutions was investigated in [21] as well, but in the nanosized crystals based on ZrO_2, the possibility of about 20 mol.% Fe_2O_3 solubility at 900 °C was pointed out.

The work [22] presents a survey of information about phase relations in the UO_2–ZrO_2 system. Fig. 3 shows the phase diagrams from [23–30]. It is worth noting that there are quite significant differences of data published in [28,29] on mutual component solubility in the solid state.

The eutectic-type phase diagrams in the vicinity of the eutectic temperature and below for the UO_{2+x}–$FeO_{1.5}$ (T_{eut} = 1240–1348 °C) and ZrO_2–$FeO_{1.5}$ (T_{eut} = 1525 °C) systems (Figs. 1 and 2) and at temperatures below 1600 °C for the UO_2–ZrO_2 system (Fig. 3) indicate limited mutual solubility. In addition the eutectic composition in the ZrO_2–$FeO_{1.5}$ and UO_{2+x}–$FeO_{1.5}$ systems is shifted towards the $FeO_{1.5}$ apex. Both these facts enable us to assume that the ternary eutectic is located in the ferrite-enriched domain of the $FeO_{1.5}$–UO_{2+x}–ZrO_2 system. Taking the data on $FeUO_4$ and FeU_3O_{10} compound formation in air [12–16] into account, it is possible to assume that several eutectic-type fields of crystallization could occur in the $FeO_{1.5}$–UO_{2+x}–ZrO_2 system.

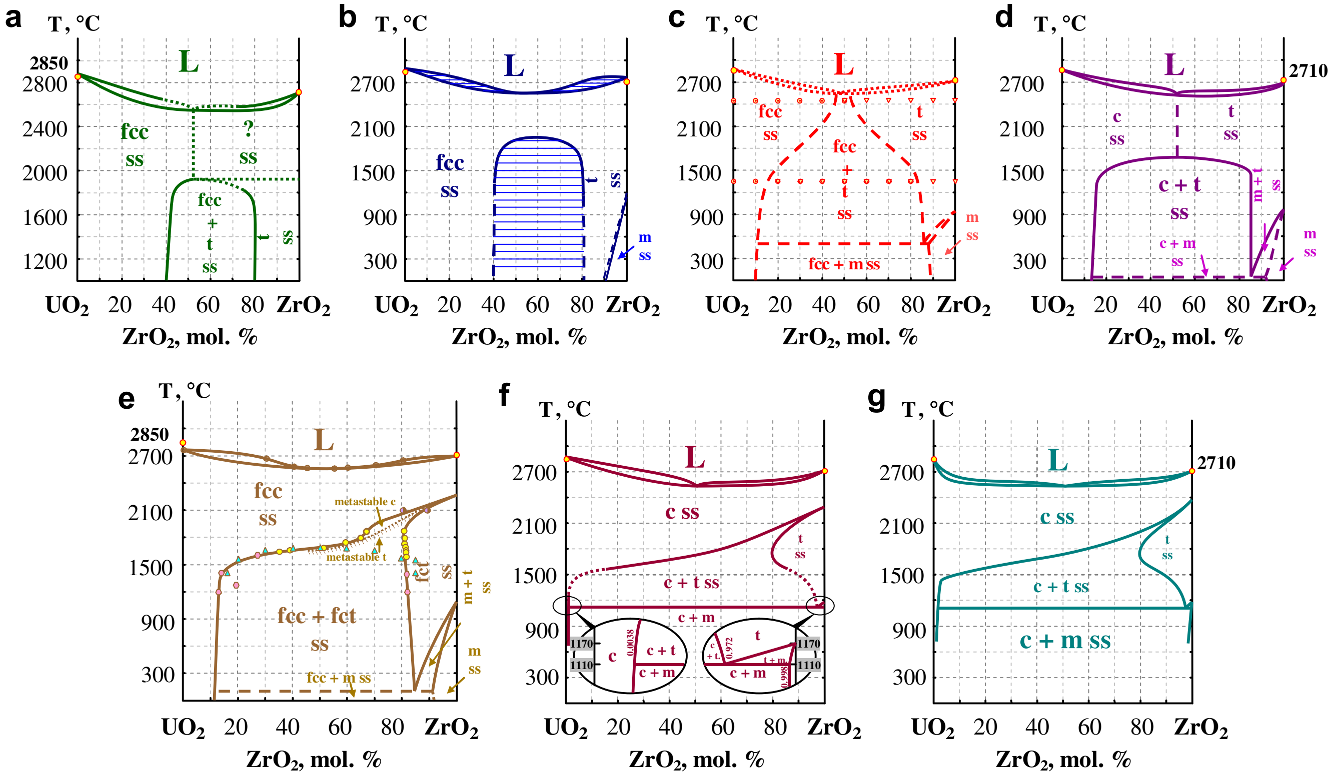

Fig. 3. Phase diagrams of the UO_2–ZrO_2 system. Literature data: (a) [23], (b) [24], (c) [25], (d) [26,27], (e) [28], (f) [29], (g) [30].

2. Materials and methods

The specimens were prepared from Fe_2O_3 (>98.1 mass%, the sum of sulphates, Cu, K, Na, Ca, Mg, Si, N < 0.6 mass%), ZrO_2 + HfO_2 (>99.3 mass% purity), UO_2 (>99.0 mass% purity, ZrO_2 < 0.9 mass%, the sum of Fe, As, CuO, phosphates, chlorides < 0.07 mass%).

A mixture of the initial components was subjected by induction melting in a cold crucible (IMCC) [31] in air at 1520 °C. After holding at 1360 ± 10 °C to homogenize the structure and establish equilibrium with the gas phase (air, $p_{O_2} = 0.21 \times 10^5$ Pa) the melt was slowly cooled.

As the $FeUO_4$ compound formed in the Fe_2O_3–UO_2–O_2 system, according to the results of Ref. [15], will decompose into Fe_2O_3 and $UO_{2.6}$ below 840 °C, the synthesis of the compound was carried out at 1200 °C [12]. There was a 2 h annealing at 1220 °C, i.e. slightly above the $FeUO_4$ phase formation. There would probably be a partial decomposition of the compound as well as oxidation of Fe^{2+} in the sample.

The microstructure, the element composition of distinct sample domains and the composition of separate phases formed after the melt crystallization were analyzed by scanning electron microscopy (SEM) and energy-dispersive X-ray spectrometry (EDS) using the ABT-55 microscope coupled with an Oxford Link microprobe

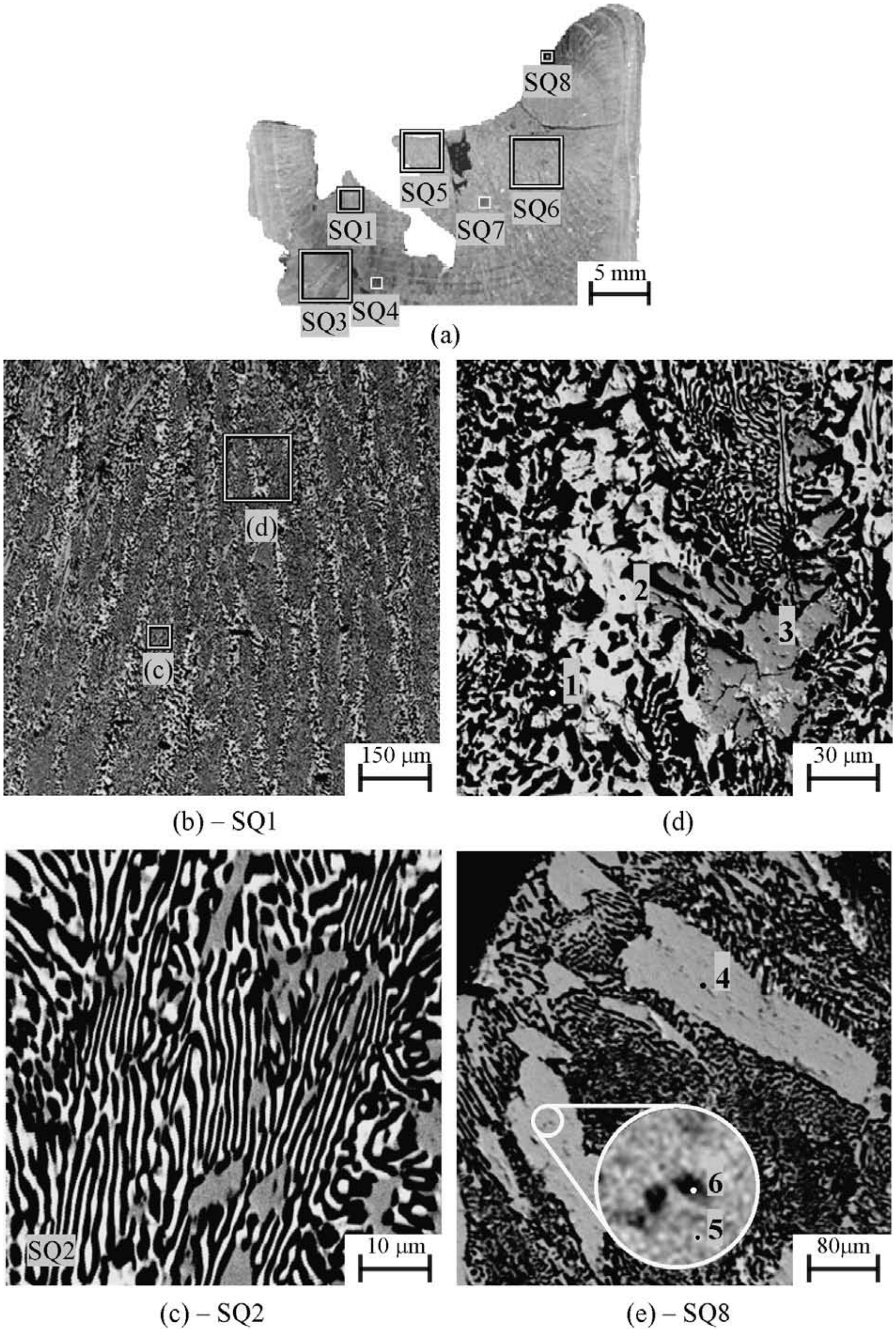

Fig. 4. The general view (a), micrographs of the eutectic zone (b)–(d) and outlying zone (e) of the sample obtained by crystallization of the 68.9 $FeO_{1.5}$, 29.0 UO_{2+x}, 2.1 ZrO_2 mol.% melt.

analyzer. The error in determining the elements content by this technique varies with the atomic number and equals ±0.3 mass% on average. In this work the EDS analysis was carried out only for cations.

For differential thermal analysis (DTA) fragments of eutectic zone were cut from the ingot after melt cooling. The eutectic zone was determined by electron microscopy. Thermal transformations in the system were studied by DTA using the SETSYS Evolution-2400. In DTA measurements, the mass of the specimen was about 10 mg, heating rate was 10 °C/min in air ($p_{O_2} = 0.21 \times 10^5$ Pa). The onset point of the peaks was identified from the intersection of the tangents extrapolated from the baseline and from the thermal effect curve. The error of the phase transformation temperatures measured by this thermal analyzer was ±0.5 °C.

The phase composition of the specimens was checked by X-ray powder diffraction (XRD) using the DRON-3 X-ray diffractometer with the Cu Kα-radiation (λ = 154.178 pm).

The oxygen content of the phases in the sample was not measured, but was fixed by experimental conditions, namely by the predetermined partial pressure of oxygen in a gas phase and temperature.

3. Results and discussion

As explained above, the sample of 68.9 $FeO_{1.5}$, 29.0 UO_{2+x}, 2.1 ZrO_2 (mol.%) nominal composition (in the ferric oxide (III)-enriched domain) was obtained by two-step cooling of the melt, first from 1520 °C down to 1360 ± 10 °C with 40 min holding time at this temperature for melt homogenization and then by slow cooling down until its crystallization. The microstructure, phase and chemical composition of the sample are presented in Fig. 4 and in Table 1. The typical microstructure of eutectic crystallization is observed in the central zone of the sample (Fig. 4). The chemical composition of all the measured zones (Table 1) is almost the same, this confirms their homogeneous character on the macroscopic scale.

However the phase composition of the phases within the individual eutectically crystallized zones shows considerable variation. There are $FeO_{1.5}$-based phases (Fig. 4 and region 1, Table 1), UO_{2+x}-based phases (Fig. 4 and region 2, Table 1) and finally mixed $U(Zr)FeO_{4-\delta}$ phases (Fig. 4 and regions 3 and 4, Table 1). The $FeO_{1.5}$ phase shows extremely low solubility of the UO_{2+x} and ZrO_2 (region 1, Table 1) although overestimation of the UO_{2+x} and ZrO_2 contents is possible due to small size (Fig. 4) of the $FeO_{1.5}$-based grains – a limitation of the EDS technique. In the grains based on UO_{2+x} a small content of the ferric and zirconium oxides was found (region 2, Table 1), again these values may also be underestimated given the small spot size. The third type of grain in the sample consists mainly of ferric and uranium oxides and some zirconia as a solid solution (Fig. 4 and regions 3, 4, Table 1). According to the element ratios, a stoichiometry of this phase is close to the $UFeO_4$ compound and could be considered as a $U(Zr)FeO_4$ solid solution.

Table 1
The results of EDS analysis of the domains marked in Fig. 4.

Examined region	$FeO_{1.5}$	UO_{2+x}	ZrO_2
	mol.%		
SQ1	67.3	30.5	2.1
SQ2	67.5	30.3	2.2
SQ3	67.6	30.0	2.4
SQ4	67.5	30.4	2.1
SQ5	69.2	29.0	1.8
SQ6	66.7	31.5	1.8
SQ7	66.1	31.9	2.0
1	98.8	0.6	0.6
2	3.2	95.7	1.1
3	41.0	52.1	7.0
4	40.7	51.1	8.2

Note: oxygen content was not determined by EDS analysis (stoichiometric composition is given using the cations content determined by EDS).

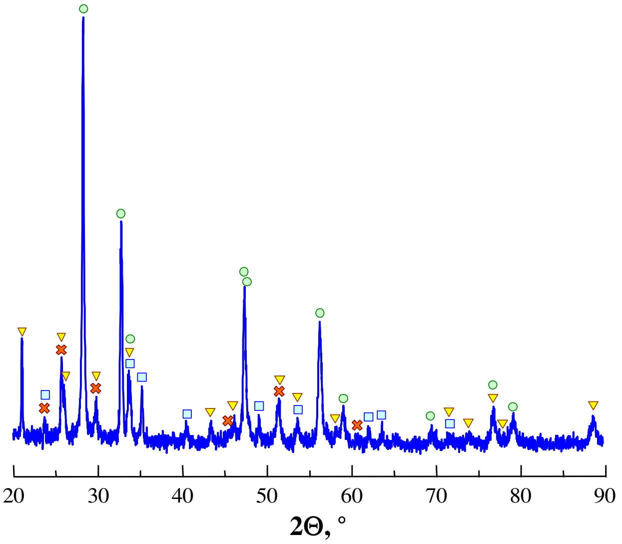

Fig. 5. X-ray powder pattern of the specimen cut off from the eutectic zone in the $FeO_{1.5}$–UO_{2+x}–ZrO_2 system. ○, *t*-U_3O_7-based phase (15–4); ▽, *ortho*-U_3O_8-based phase (2–276); ✖, *ortho*-$UFeO_4$-based phase (39–200); □, *rhomb*-Fe_2O_3 (1–1053, hematite).

The phase composition of the eutectic zone (Fig. 4, region SQ3) was also determined by XRD (Fig. 5). The main phase crystallized in the eutectic zone is a U_3O_8-based phase. In addition the peaks of Fe_2O_3 (hematite-type structure) are presented. The strongest peaks of the $UFeO_4$ compound overlap with the main peaks of U_3O_8 and Fe_2O_3, and only weak peaks of $UFeO_4$ are distinctive (d = 0.19714 and 0.15359 nm, 2θ = 46.0 and 60.2°, respectively, Fig. 5). Nevertheless these indicate the presence of the compound in the sample. The formation of a large quantity of the U_3O_7-based solid solution, which melts at the lower temperature than U_3O_8 (Fig. 5), is associated very likely with solid state decomposition of the $U(Zr)FeO_4$-based solid solution (which is inhomogeneous

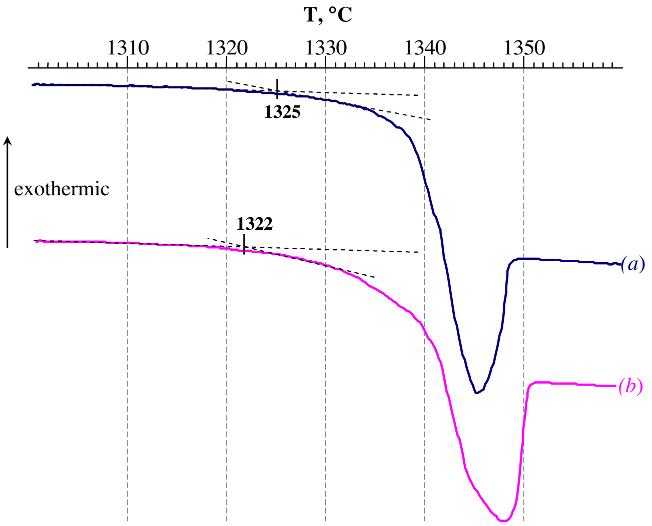

Fig. 6. DTA curve of the specimens cut off from the eutectic zone in the $FeO_{1.5}$–UO_{2+x}–ZrO_2 system: (a) fragment of the SQ3 domain (Fig. 4), (b) fragment of the SQ5 domain (Fig. 4).

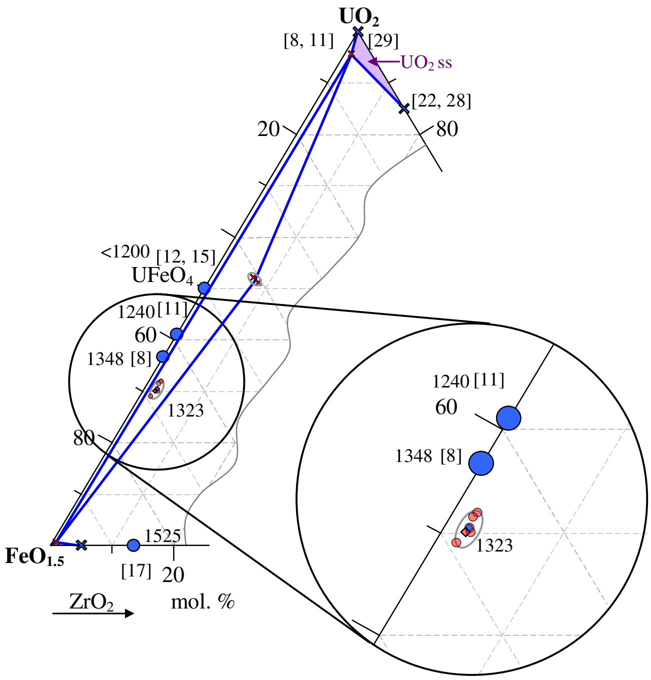

Fig. 7. Phase relations in the $FeO_{1.5}$–ZrO_2–UO_{2+x} system at 1323 °C (eutectic temperature) in air. ◆, initial composition in the system under consideration; ●, eutectic, ✖, composition of the coexisting solid phases, ◯, area of the root-mean-square deviations of the experimental results, ▨, solid solution domain, —, tie-lines.

with respect to the oxygen and iron) to the Fe_2O_3 and U_3O_7-based solid solutions. This assumption enables to explain not only the large quantity of the U_3O_7-based phase, but also a small content of the $UFeO_4$-based phase in the sample compared to the location of the melt's nominal composition in the Fe_2O_3–$U(Zr)FeO_{4-\delta}$–UO_{2+x} subsystem. The SEM results show the heterogeneous composition of the grains of the $UFeO_4$-based solid solution and also support this assumption. There are also darker inclusions inside the grains, which probably are the products of the compound decomposition (U_3O_7 – light domains and Fe_2O_3 – dark domains, Fig. 4, *e*, region 5 and region 6, respectively).

To define the eutectic temperature the DTA method was used. The DTA curves of the sample cut off from the eutectic zone are presented in Fig. 6. The asymmetric form of endothermic peaks is most likely connected with the beginning of interaction of corundum crucible with the liquid phase that appeared during the experiment. Fig. 6(b) shows that two endothermic processes are observed. This fact is most likely connected with a small deflection of composition accordingly the eutectic point. But, the temperature of occurrence of a liquid phase in the system is of importance. The eutectic temperature was chosen as the value where the tangent to the base line meets the tangent to the gentle slope of first endothermic peak. According to these curves the eutectic temperature can be accepted as equal to 1323 ± 7 °C.

The compositions of the phases crystallized at the eutectic temperature and composition determined by SEM are presented in the $FeO_{1.5}$–UO_{2+x} segment of the phase diagram, Fig. 7 along with the data of others. The results correspond well with that of the neighboring point particularly the eutectic temperature of 1348 °C for the 64 mol.% $FeO_{1.5}$–36 mol.% UO_{2+x} solid solution [8].

4. Conclusions

The temperature and the composition of the ternary eutectic were determined as the following values: 1323 ± 7 °C and 67.4 ± 1.0 $FeO_{1.5}$, 30.5 ± 1.0 UO_{2+x}, 2.1 ± 0.2 ZrO_2 mol.% for the $FeO_{1.5}$–UO_{2+x}–ZrO_2 system in air. The composition of the UO_{2+x} ($FeO_{1.5}$, ZrO_2) solid solution at the eutectic temperature is 95.7 UO_{2+x}, 3.2 $FeO_{1.5}$ and 1.1 ZrO_2 mol.%. The solubilities of UO_2 and ZrO_2 in $FeO_{1.5}$ do not exceed 0.6 mol.% at the eutectic temperature. The ZrO_2 solubility in $UFeO_4$ at the eutectic temperature of 1323 ± 7 °C corresponds to 7.0 mol.%.

Moreover, it is necessary to note that the results obtained in the present investigation showed the importance of more detailed study of pseudo-binary sections and ternary sub-systems of $FeO_{1.5}$–UO_{2+x}–ZrO_2 system. Studying the region of existence of the $UFeO_4$-based compound is of great value. Finally the variation of oxygen potential in this system has fundamental influence and needs to be carefully scrutinized.

Acknowledgements

This work was supported by the ISTC (EU) Project #1950.2. The authors express their gratitude to Dr M. Hugon (UFR S.E.G.M.I.), Dr V.Ya. Rudneva (ISTC) and Dr Yu.N. Aniskevich (NITI) for the research coordination, the engineers A.V. Lysenko, V.R. Bulygin, R.A. Kosarevsky and Dr S.Yu. Kotova (NITI) for their activity in the IMCC and DTA experimental work, M.D. Tolkachev (IPGG RAS) for SEM/EDS analysis.

References

[1] H. Tuomisto, T.G. Theofanous, Nucl. Eng. Des. 148 (1994) 171.
[2] S.V. Bechta, V.B. Khabensky, S.A. Vitol, et al., Nucl. Eng. Des. 236 (2006) 1810.
[3] S.V. Bechta, V.B. Khabensky, S.A. Vitol, et al., Nucl. Eng. Des. 236 (2006) 1362.
[4] V.V. Gusarov, V.I. Almjashev, V.B. Khabensky, S.V. Beshta, V.S. Granovsky, Glass Phys. Chem. 31 (1) (2005) 53.
[5] V.B. Khabensky, V.S. Granovsky, S.V. Beshta et al., Chinese Patent ZL 2004 1 0031091.1, Date of Publication March 14, 2007. Priority of April 22, 2004.
[6] V.P. Barzakovsky, V.V. Lapin, A.I. Boykova, N.N. Kurtseva, Phase Diagrams of Silicate Systems, Reference Book, vol. 4, Ternary Oxide Systems, Nauka, Leningrad, 1974 (in Russian).
[7] B. Cheynet, P. Chaud, P.Y. Chevalier, E. Fisher, P. Mason, M. Mignanelli, J. Phys. IV 113 (2004) 61.
[8] W.D.J. Evans, J. White, Trans. Brit. Ceram. Soc. 63 (12) (1964) 705.
[9] L.S. Darken, R.W. Gurry, J. Am. Chem. Soc. 67 (1945) 1398.
[10] L.P. Mezentseva, V.F. Popova, V.I. Almjashev, N.A. Lomanova, V.L. Ugolkov, S.V. Beshta, V.B. Khabensky, V.V. Gusarov, Russ. J. Inorg. Chem. 51 (1) (2006) 118.
[11] B. Riley, Trans. Am. Nucl. Soc. 12 (1969) 543.
[12] W. Rudorff, H. Erfurth, S. Kemmler-Sack, Z. Anorg. Allg. Chem. 354 (5–6) (1967) 273.
[13] A. Collomb, J.J. Capponi, M. Gondrand, J.C. Joubert, J. Solid State Chem. 23 (3–4) (1978) 315.
[14] L.M. Kovba, G.P. Polunina, V.N. Verbetskiy, E.S. Bikbulatov, MSU Bull. Ser. Chem. 2 (6) (1966) 29. in Russian.
[15] H.R. Hoekstra, R.H. Marshall, Adv. Chem. 71 (1967) 211.
[16] D. Labroche, J. Rogez, J.P. Laval, O. Dugne, in: Proceedings of the 10th International IUPAC Conference, 10–14 April 2000, Julich, Germany, vol. 15, Part 1, pp. 89.
[17] T.S. Jones, Sh. Kimura, A. Muan, J. Am. Ceram. Soc. 50 (3) (1967) 137.
[18] Yu.B. Petrov, M. Kiselova, SARNET Project Results, 2004–2006 (private communications).
[19] Yu.B. Petrov, Yu.P. Udalov, J. Slovak, Yu.G. Morozov, Glass Phys. Chem. 28 (3) (2002) 139.
[20] J.F. Collins, I.F. Ferguson, J. Chem. Soc. A (1) (1968) 4.
[21] S. Music, S. Popovic, B. Grzeta, G. Stefanic, I. Gzako-Nagy, J. Alloy. Compd. 241 (1&2) (1996) 10.
[22] V.I. Almjashev, M. Barrachin, S.V. Bechta, D. Bottomley, F. Defoort, M. Fischer, V.V. Gusarov, S. Hellmann, V.B. Khabensky, E.V. Krushinov, D.B. Lopukh, L.P. Mezentseva, A. Miassoedov, Yu.B. Petrov, S.A. Vitol, JNM, 2009, submitted for publication.
[23] W.A. Lambertson, M.H. Mueller, J. Am. Ceram. Soc. 36 (1953) 365.
[24] G.M. Wolten, J. Am. Chem. Soc. 80 (1958) 4772.
[25] P.E. Evans, J. Am. Ceram. Soc. 43 (1960) 443.
[26] N.M. Voronov, E.A. Voytekhova, I.T. Kovalev, in: Structures of Alloys in Some Systems Containing Uranium and Thorium (transactions of the A.A. Baykov, Institute of Metallurgy RAS), Gosatomizdat, Moscow, 1961, p. 467 (in Russian).
[27] N.M. Voronov, R.M. Sofronova, E.A. Voytekhova, High-Temperature Chemistry of Uranium Oxides and Their Compounds, Atomizdat, Moscow, 1971 (in Russian).
[28] J. Cohen, B.E. Schaner, J. Nucl. Mater. 9 (1) (1963) 18.
[29] C.F. Baes, J.H. Shaffer, H.F. McDuffie, Trans. Am. Nucl. Soc. 6 (2) (1963) 393.
[30] P.D. Bottomley, M. Coquerelle, Nucl. Technol. 87 (1989) 120.
[31] Yu.B. Petrov, Induction Melting of Oxides, Energatomizdat Publishers, Leningrad, Leningrad Branch, 1983 (in Russian).